Eur. Phys. J. E (2017) **40**: 39
DOI 10.1140/epje/i2017-11530-8

THE EUROPEAN PHYSICAL JOURNAL E

Regular Article

Spontaneous imbibition in parallel layers of packed beads

S. Ashraf[1], G. Visavale[1], S.S. Bahga[2], and J. Phirani[1,a]

[1] Department of Chemical Engineering, Indian Institute of Technology Delhi, Hauz Khas, New Delhi, 110016, India
[2] Department of Mechanical Engineering, Indian Institute of Technology Delhi, Hauz Khas, New Delhi, 110016, India

Received 16 December 2016 and Received in final form 15 February 2017
Published online: 5 April 2017 –

Abstract. The imbibition of a wetting fluid in a homogeneous porous medium follows the diffusion-like behavior described by Washburn. The impregnation of a two-layered porous medium by a wetting fluid due to capillary action has been previously described to have two fronts, one saturating the medium and the other, leading front, which propagates in finer pores. Here, we report that the leading front is governed by the porous structure and is not always in the finer pores. Based on the experiments in a layered porous medium of permeability varying perpendicular to the direction of flow, we show that the permeability of the adjacent layers plays a significant role in determining the leading front amongst the layers. We have also developed an analytical model which describes the flow dynamics in the layered porous medium. The model predicts the condition for which the leading front in the larger pores is followed by the front in the finer pores. This condition is also verified experimentally.

1 Introduction

The flow of viscous fluids in porous media due to capillary forces is of great importance in the fields of enhanced oil recovery [1,2], geological CO_2 sequestration [3,4], fabric design [5], chemical reactors [6] and medical diagnostics [7]. Lucas [8] and Washburn [9] gave a lubrication approximation model, showing the diffusive dynamics of imbibed length l of a perfectly wetting fluid of viscosity μ, surface tension γ with time t as $l^2 = (\frac{d\gamma}{4\mu})t$, in a capillary of diameter d. It is important to note that fluid traverses more distance in a larger diameter capillary, in the same time interval t because the permeability is proportional to d^2 and the capillary force is proportional to $\frac{1}{d}$. Several modifications to Washburn's law for diffusive dynamics have been reported for different cross-section shapes of capillary [10–12], axially varying geometries [13, 14] and in the presence of a viscous non-wetting fluid in the capillary [15–18] showing that the meniscus displacement deviates from Washburn's law ($l^2 \propto t$).

The spontaneous imbibition due to capillary forces in a homogenous porous medium has also been shown to follow the diffusion-like response described by Washburn. This is because the permeability of a porous medium is directly proportional to the square of the particle diameter according to the classical Kozeny-Carman model [19], whereas the capillary pressure is inversely proportional to the particle diameter [6,20]. This is analogous to the relationship between the permeability and Young-Laplace pressure in a capillary and explains the observed Washburn-like behavior seen in the porous media. The front displacement square is also proportional to the particle diameter of a homogeneous porous medium. Reyssat *et al.* [20] showed that the diffusive dynamics vary in a porous medium with permeability varying in the direction of flow. Bico and Quéré [21] and Dong *et al.* [22] showed that in a bi-disperse medium, fluid rise is more in the layer of narrow channels and this is attributed to the fluid transfer from large channels to narrow channels. Bico and Quéré [21] also showed that the front measured by the weight imbibed and the visible front in the finer pores, both follow the diffusive law.

In this work we explore spontaneous imbibition and its dynamics in layered porous media using experiments and a one-dimensional lubrication approximation model. Our experiments show that different imbibition patterns emerge in a layered porous medium for a capillary-driven flow. The leading front of the imbibing fluid is not always in the narrow channels and is dependent on the relative position and permeability of the layers. Our one-dimensional model is able to explain the conditions for which the leading front is not in the narrowest channel. At very early time scales, the inertial effects are also important [23–25]. However, the inertial time scales in the present work are of the order of 1 milisecond and can be neglected for the time scales used in the model and in the experiments. We also show that the sum of squares of the individual lengths imbibed in the layers is proportional to time, rather than the square of the total volume imbibed being proportional to time.

[a] e-mail: jphirani@chemical.iitd.ac.in

2 Experiments and analytical model

2.1 Two-layered porous medium

A porous medium is constructed using a pair of microscopic glass slides of length 75 mm, placed 1 mm apart. Three glass bead sizes of diameter 0.1 mm, 0.5 mm and 1 mm are used to construct the porous media. The glass beads are washed with acetone and rinsed several times to remove the impurities adhearing onto the beads. Three separate porous media having two layers are constructed using i) 0.1 mm and 0.5 mm, ii) 0.5 mm and 1 mm and iii) 0.1 mm and 1 mm diameter beads as shown in fig. 1. The width of the slides used in these cases is 16 mm (8 mm for each layer). The layers are continuous and can hydrodynamically communicate with each other through the pore spaces. A reservoir is constructed on one end of the model and paraffin oil is filled in the reservoir, which is the wetting phase and imbibes into the porous medium. The viscosity of the paraffin oil is 0.056 Pa s, the surface tension is 0.0206 N m^{-1}, and the density is 875 kg m^{-3}. The other end of the porous medium is left open for outflow. A high-resolution camera (Nikon D 750) is used for recording the imbibition phenomena and a customized image analysis software in MATLAB is used for image analysis. The front displacement snapshots and length *vs.* time graphs of the three cases are shown in fig. 1(a), (b), (c). For the two-layered media, the fluid front displacement is always more in the smaller permeability layer of the two layers, for all the three arrangements. This is in agreement with the results by Bico and Quéré [21].

We now use a one-dimensional lubrication approximation model to explain the pattern of the observed front displacement. We assume that for a layered porous medium formed by beads of diameters d and D ($d < D$), the layers have permeability $k = \Lambda d^2$ and $K = \Lambda D^2$. This scaling for permeability holds for small beads, where Λ can be estimated by the Kozeny-Carman equation [19]. On the other hand, for large beads which are of the size of gap between the top and the bottom walls, the same scaling is valid. This is because for large beads, even the gap between the top and the bottom walls scales with the diameter of the beads. However, we note that Λ in such a case cannot be estimated by the Kozeny-Carman equation. The order of magnitude of Λ is assumed to be same for the single layer of beads, as the resistance offered by the beads is similar. Therefore, same Λ is used in developing the one-dimensional model.

The front displacements of a completely wetting fluid of viscosity μ and surface tension γ are l and L, respectively, at time t ($l > L$), as shown in fig. 2(a). The viscous loss in the large permeability layer is given by Darcy's equation as

$$P(L,t) - P_0 = -\frac{\mu U L(t)}{K}, \qquad (1)$$

where U is the velocity of the fluid in the large permeability layer (K), P_0 is the atmospheric pressure, and u is the velocity of the fluid in the small permeability layer

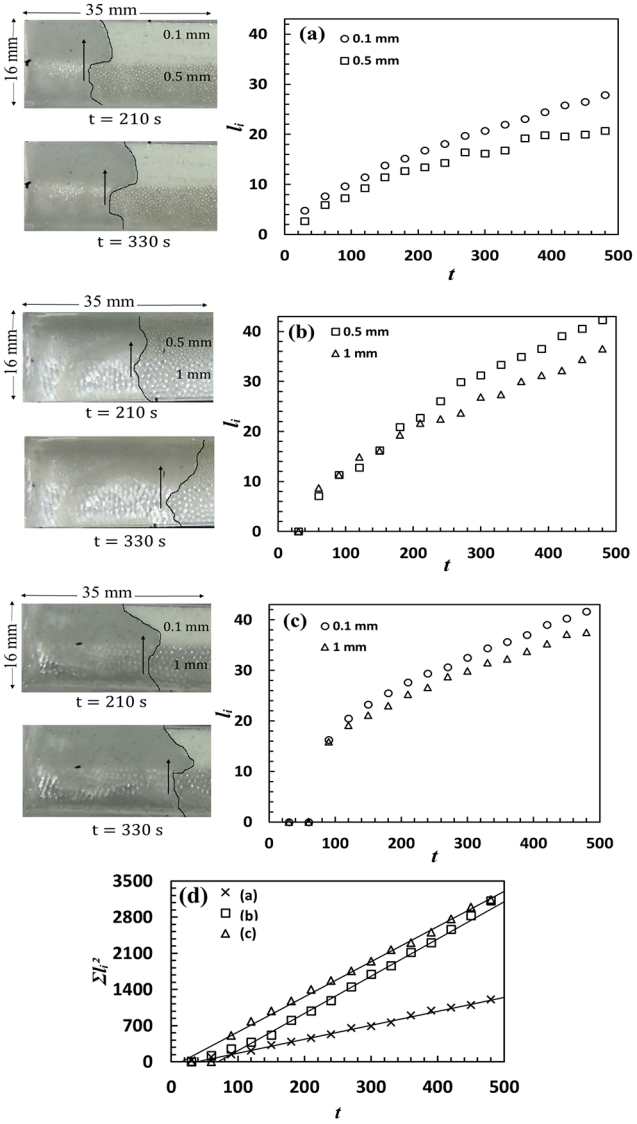

Fig. 1. Interacting two-layered porous media. The images of porous media show the imbibition at different times. The fluid exchange between the layers is represented by arrows in the snapshots. (a), (b) and (c) show the different cases for a two-layered porous media made of 0.1 mm, 0.5 mm, and 1 mm glass beads. The l_i (mm) *vs.* t (s) graphs show the experimental data for each of the arrangements. (d) shows the sum of squares of imbibed lengths ($\sum l_i^2 = L^2 + l^2$) in mm^2 *vs.* time in s for the cases (a), (b) and (c). The slopes for the lines shown in (d) for the cases (a), (b) and (c) are 2.8, 7.2 and 6.8 mm^2 s^{-1}, respectively.

(k) till L. We now hypothesize that for length L, the pressure gradient in both the layers is same which implies $\frac{U}{K} = \frac{u}{k}$, and fluid transfer happens between the adjoining layers only at the front assuming lubrication approximation. The fluid from the large permeability layer goes to the small permeability layer at the front [21], increasing the flow rate in the latter after the front at L. The viscous loss in the small permeability layer after the transfer dq

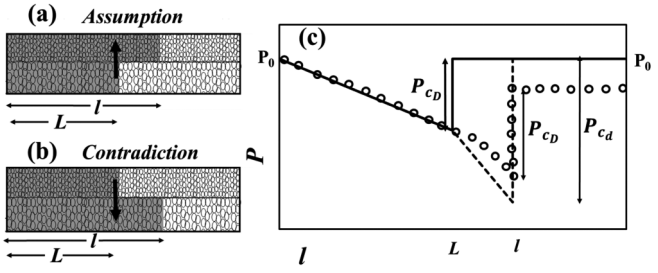

Fig. 2. (a) A schematic of the fluid transfer from the large permeability layer to the small permeability layer. (b) A schematic of the fluid transfer from the small permeability layer to a large permeability layer which is a contradiction. (c) Pressure *vs.* distance graph. The solid and the dashed lines represent the large and the small permeability layers shown in the case (a); the circles represent the large permeability layer shown in case (b).

can be written as

$$P(l,t) - P(L,t) = -\frac{\mu(l-L)}{k}\left(u + \frac{dq}{A}\right), \tag{2}$$

where A is the area of the cross-section. The velocities of the fluid fronts after the fluid transfer are

$$\phi\frac{\mathrm{d}L}{\mathrm{d}t} = U - \frac{dq}{A}, \tag{3}$$

$$\phi\frac{\mathrm{d}l}{\mathrm{d}t} = u + \frac{dq}{A}, \tag{4}$$

where ϕ is the porosity of the layers. The Young-Laplace equation for pressure drop in the two layers is

$$P(L) - P_0 = -\frac{c\gamma}{D}, \tag{5}$$

$$P(l) - P_0 = -\frac{c\gamma}{d}, \tag{6}$$

where c is a constant. These equations for l and L with time reduce to

$$\left(\frac{c\gamma\Lambda}{\phi\mu}\right)\frac{D^2+d^2}{D} = L\left(\frac{\mathrm{d}L}{\mathrm{d}t} + \frac{\mathrm{d}l}{\mathrm{d}t}\right), \tag{7}$$

$$\left(\frac{c\gamma\Lambda}{\phi\mu}\right)\frac{d}{D}(D-d) = (l-L)\frac{\mathrm{d}l}{\mathrm{d}t}. \tag{8}$$

Equation (8) explains that the leading front will always be in the small permeability layer. Because $(\frac{c\gamma\Lambda d(D-d)}{\phi\mu D})$ is always positive and $(\frac{\mathrm{d}l}{\mathrm{d}t})$ is also positive during the imbibition process, so $l > L$. This can also be explained by considering the pressure drop in the layers as shown in fig. 2. Till L, the pressure and the pressure gradient in both the layers is same. We now suppose that the fluid front has moved ahead in the large permeability layer as shown in fig. 2(b). In the small permeability layer, the pressure after the front at L will be atmospheric pressure as shown in fig. 2(c). The large permeability layer has the fluid flowing from L to l also and the pressure drops further till l as shown by circles in the graph of fig. 2(c). After the front at l in the large permeability layer, the pressure should be atmospheric for which the larger permeability layer must have a higher capillary pressure than the small permeability layer. This is a contradiction and proves that the front will always be ahead in the small permeability layer in the two-layered system as shown in fig. 2(a).

Adding eqs. (7) and (8), we get

$$\frac{c\gamma\Lambda}{\phi\mu}(d+D) = \frac{1}{2}\frac{\mathrm{d}}{\mathrm{d}t}(L^2+l^2). \tag{9}$$

Equation (9) shows that the sum of squares of the lengths imbibed is proportional to the time of imbibition as shown in fig. 1(d). This shows that in a layered porous medium $(l^2+L^2) \propto \sum(Volume)^2 \propto t$, whereas in a homogeneous porous medium the square of the total volume imbibed is proportional to time. For each of the cases (a), (b), (c) shown in fig. 1, the value of the constant $(\frac{2c\gamma\Lambda}{\phi\mu})$ is 4.6, 4.8, 6.1 mm s^{-1} respectively. Equation (9) is applicable when the constant Λ used in calculating the permeability is same for all the layers irrespective of the bead diameters. Although the diameter of the large (1 mm) bead packing scales with the wall spacing, the Λ for the large beads is slightly different from that of layers of the small (0.1 mm) and the medium (0.5 mm) beads. We now evaluate the order of magnitude of the constant $(\frac{2c\gamma\Lambda}{\phi\mu})$. In all the layers, c has an order of magnitude $(\sim)1$ [20], and $(\frac{\gamma}{\mu}) \sim 10^3$ mm s^{-1}. Λ for all the layers is different because the Kozeny-Carman equation cannot be used when the bead diameter is the same as the spacing between the glass plates. But the order of magnitude of Λ can be determined by the Kozeny-Carman equation which is 10^{-4}, for a porosity of 0.3, measured for all the beads. This implies that the order of magnitude of $(\frac{2c\gamma\Lambda}{\phi\mu})$ is 1 mm s^{-1} as evaluated for the three cases in fig. 1.

2.2 Three-layered porous medium

To make a three-layered porous medium, the beads are filled layer-by-layer for a width of 8 mm each. All the three possible combinations of the interacting layers are considered for a three-layered system as shown in fig. 3. Spontaneous imbibition experiments are carried out and the displacement of the fluid fronts with time is shown in fig. 3. In the arrangements shown in fig. 3(a), (b), we observe that the fluid front is ahead in the small permeability layer, which is similar to the results of the two-layered system. However, in fig. 3(c), the fluid front is ahead in the medium permeability layer.

To model this anomalous behavior, we assume that the fluid transfer happens from the large permeability layer to the adjacent small permeability layer(s) at the front only, as shown in fig. 3 by arrows in the snapshots. We use Darcy's law in each section between the fronts to arrive at the pressure drop. The total suction pressure in each layer is given by the Young-Laplace equation. Then proceeding as in the two-layered case, for arrangements in fig. 3(a), (b), the governing equations for the rate of front

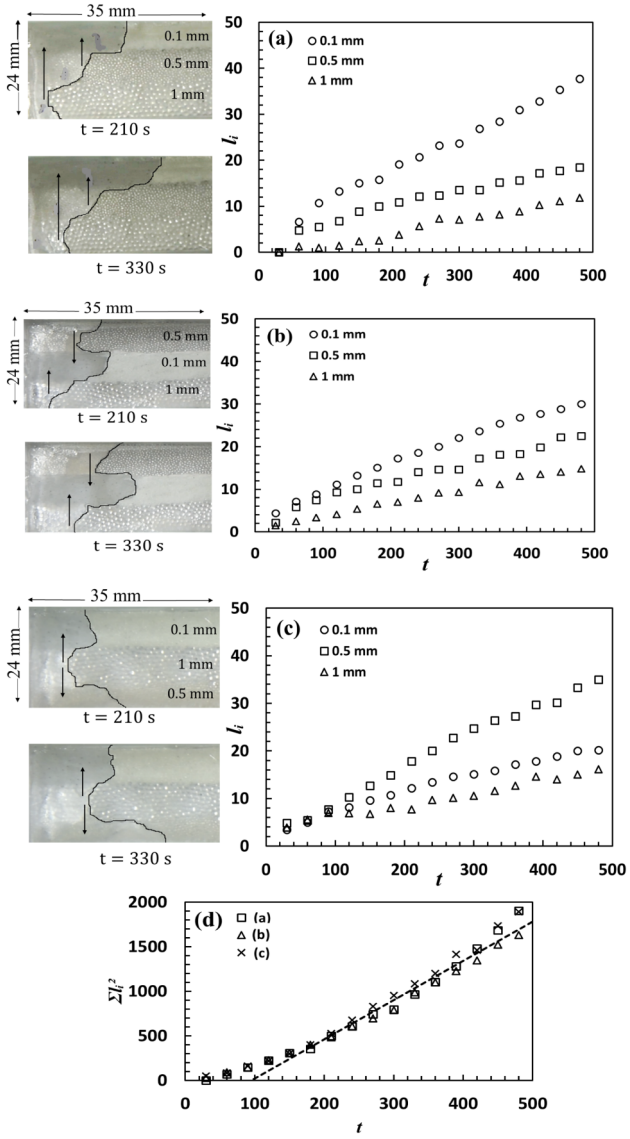

Fig. 3. Interacting three-layered porous media. The images of the porous media show the imbibition at different times. The fluid exchange among the layers is represented by arrows in the snapshots. (a), (b) and (c) show the different arrangement of layers in three-layered porous media made of 0.1 mm, 0.5 mm, and 1 mm glass beads. The l_i (mm) *vs.* t (s) graphs show the experimental data for each of the arrangements. (d) The slope of the sum of squares of imbibed lengths ($\sum l_i^2 = L^2 + l_m^2 + l^2$) in mm^2 *vs.* time in s for the arrangements in (a), (b) and (c) is 4.4 mm^2 s^{-1}.

displacement in different layers are given by

$$\frac{D^2+d_m^2+d^2}{D}\frac{c\gamma\Lambda}{\phi\mu} = L\left(\frac{\mathrm{d}L}{\mathrm{d}t}+\frac{\mathrm{d}l_m}{\mathrm{d}t}+\frac{\mathrm{d}l}{\mathrm{d}t}\right), \quad (10)$$

$$(d_m^2+d^2)\left(\frac{1}{d_m}-\frac{1}{D}\right)\frac{c\gamma\Lambda}{\phi\mu} = (l_m-L)\left(\frac{\mathrm{d}l_m}{\mathrm{d}t}+\frac{\mathrm{d}l}{\mathrm{d}t}\right), \quad (11)$$

$$\frac{d}{d_m}(d_m-d)\frac{c\gamma\Lambda}{\phi\mu} = (l-l_m)\frac{\mathrm{d}l}{\mathrm{d}t}, \quad (12)$$

where $d = 0.1$ mm, $d_m = 0.5$ mm and $D = 1$ mm and l, l_m and L are the fluid front positions in the small ($k = \Lambda d^2$), the medium ($k_m = \Lambda d_m^2$) and the large ($K = \Lambda D^2$) permeability layers, respectively, at time t. Adding eqs. (10), (11), and (12) for the arrangements shown in fig. 3(a), (b) we get

$$(D+d_m+d)\frac{c\gamma\Lambda}{\phi\mu} = \frac{1}{2}\frac{\mathrm{d}}{\mathrm{d}t}\left(L^2+l_m^2+l^2\right). \quad (13)$$

Figure 3(d) shows that eq. (13) is satisfied by the experiments, *i.e.* $(l^2+l_m^2+L^2) \propto \sum(Volume)^2 \propto t$ with a slope of $(D+d_m+d)\frac{2c\Lambda\gamma}{\phi\mu} = 4.4\,\mathrm{mm^2\,s^{-1}}$. As the velocities in all the layers are positive during the imbibition process and the left-hand terms of the equations are also positive, it can be inferred from eq. (11) that $l > l_m$ and $l_m > L$ from eq. (12). Thus, the fluid front positions are arranged as $L < l_m < l$ at all times, which is in the order of decreasing permeability or decreasing particle diameter of the layer.

For the arrangement shown in fig. 3(c), proceeding as in the earlier case, the governing equations for the rate of front displacement with time are

$$\frac{D^2+d_m^2+d^2}{D}\frac{c\gamma\Lambda}{\phi\mu} = L\left(\frac{\mathrm{d}L}{\mathrm{d}t}+\frac{\mathrm{d}l_m}{\mathrm{d}t}+\frac{\mathrm{d}l}{\mathrm{d}t}\right), \quad (14)$$

$$(D-d_m)\frac{d_m}{D}\frac{c\gamma\Lambda}{\phi\mu} = (l_m-L)\frac{\mathrm{d}l_m}{\mathrm{d}t}, \quad (15)$$

$$\frac{d}{D}(D-d)\frac{c\gamma\Lambda}{\phi\mu} = (l-L)\frac{\mathrm{d}l}{\mathrm{d}t}. \quad (16)$$

Adding eqs. (14), (15), and (16) for the arrangement shown in fig. 3(c), we get eq. (13). Figure 3(d) suggests that the model is able to predict the capillary-driven flow behavior in arbitrarily arranged parallel layers of packed beads. The value of $(\frac{2c\gamma\Lambda}{\phi\mu})$ for three-layered porous media is 2.75 mm s^{-1} (which is again of the order 1).

Now, we try to predict the fluid front positions for the three-layered case. From eqs. (15), and (16), $L < l_m$ and $L < l$; but the relative positioning of l and l_m is still unclear. Using the hypothesis developed in the two-layered system, it is clear that the fluid transfer occurs from the large permeability layer (K) to the smaller permeability layers (k_m and k). Since the small permeability layer and the medium permeability layer are not in contact with each other, their pressure gradients can be different after L, unlike in the previous cases. We now use the pressure drop in the layers to arrive at the possible solutions of the front positions.

Figure 4(a) shows a condition where

$$\left(\frac{\mathrm{d}P}{\mathrm{d}z}\right)_d < \left(\frac{\mathrm{d}P}{\mathrm{d}z}\right)_{d_m} \quad \text{for } z > L. \quad (17)$$

Now, the front in the small permeability layer shown by the dotted line in fig. 4(a) has to travel a larger distance ($l_m \ll l$) so that $(P_c)_{d_m} < (P_c)_d$ as shown in fig. 4(a), where P_c is the capillary suction pressure. From Darcy's

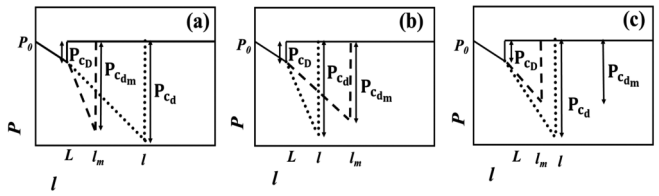

Fig. 4. Possible conditions for pressure *vs.* distance graph of an interacting three-layered porous medium.

equation, the relation between pressure gradients can be expressed as

$$\frac{\mu\phi(\frac{\mathrm{d}l}{\mathrm{d}t})}{\Lambda d^2} < \frac{\mu\phi(\frac{\mathrm{d}l_m}{\mathrm{d}t})}{\Lambda d_m^2}\,. \tag{18}$$

This condition holds true if $(\frac{\mathrm{d}l}{\mathrm{d}t}) \ll (\frac{\mathrm{d}l_m}{\mathrm{d}t})$ as $(\frac{1}{d^2}) > (\frac{1}{d_m^2})$. This implies that $l < l_m$. But $(P_c)_{d_m} < (P_c)_d$, implies $l_m < l$, which is a contradiction. This precludes the case where $(\frac{\mathrm{d}P}{\mathrm{d}z})_d < (\frac{\mathrm{d}P}{\mathrm{d}z})_{d_m}$. Now, we know that

$$\left(\frac{\mathrm{d}P}{\mathrm{d}z}\right)_{d_m} < \left(\frac{\mathrm{d}P}{\mathrm{d}z}\right)_{d}, \tag{19}$$

i.e., from Darcy's law,

$$\frac{\mu\phi(\mathrm{d}l_m/\mathrm{d}t)}{\Lambda d_m^2} < \frac{\mu\phi(\mathrm{d}l/\mathrm{d}t)}{\Lambda d^2}\,. \tag{20}$$

This condition is shown in fig. 4(b), (c) for which we explore the possible front positions. Because $(\frac{1}{d_m^2}) < (\frac{1}{d^2})$, $(\frac{\mathrm{d}l}{\mathrm{d}t})$ can be greater or less than $(\frac{\mathrm{d}l_m}{\mathrm{d}t})$ based on the bead diameter ratio. If $d_m + d = D$, the left-hand side of eqs. (15) and (16) becomes $(\frac{dd_m c\gamma\Lambda}{\phi\mu D})$ implying $l_m = l$. If $d+d_m < D$, then these equations lead to $l < l_m$ as seen in the experiment shown in fig. 3(c) for $d = 0.1\,\mathrm{mm}$, $d_m = 0.5\,\mathrm{mm}$ and $D = 1\,\mathrm{mm}$. But if $d+d_m > D$, then eqs. (14), (15) and (16) lead to $l > l_m$. Now, to prove this, we choose bead diameters of $d = 0.5\,\mathrm{mm}$, $d_m = 0.8\,\mathrm{mm}$ and $D = 1\,\mathrm{mm}$ and perform the spontaneous imbibition experiment where beads of diameter D are placed between the layers of bead diameters d_m and d as shown in fig. 5(a). The slides are kept 2 mm apart to accommodate more than 1 layer of 0.8 mm beads. In this case, the front in the small permeability layer is ahead of the front in the medium permeability layer unlike for the arrangement in fig. 3(c). The front in the large permeability layer trails the two fronts. Figure 5(b) shows that $(l^2 + l_m^2 + L^2) \propto \sum Volume^2 \propto t$. The value of $(\frac{2c\gamma\Lambda}{\phi\mu})$ for this case is $1.87\,\mathrm{mm\,s^{-1}}$. As explained in sect. 2.1, the order of magnitude of the constant $(\frac{2c\gamma\Lambda}{\phi\mu})$ is 1 for all the cases described in the three-layered porous media.

The condition of $d + d_m > D$ gives a very narrow range of diameters unlike the heterogeneity encountered in the real situations. For the condition $d + d_m < D$, the front displacement in the arrangement of fig. 3(c) shows an anomalous behavior. So, for the three-layered system we prove that the leading front is not always present in the small permeability layer.

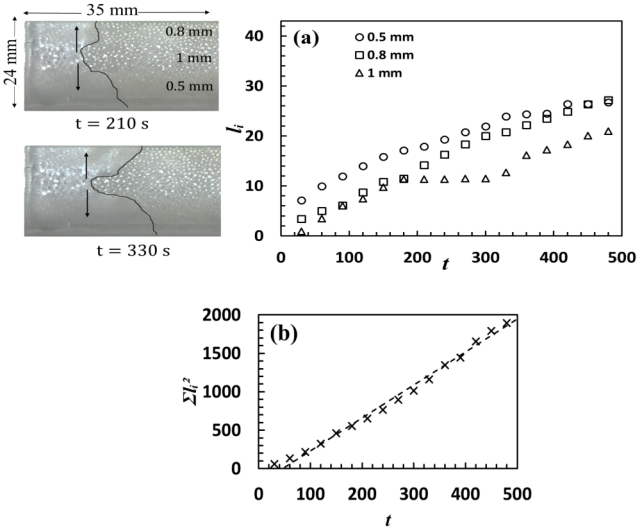

Fig. 5. The porous medium is made of bead diameters 0.5 mm, 0.8 mm, and 1 mm. The positioning of layers is the same as in fig. 3(c). (a) The l_i (mm) *vs.* t (s) graphs show the experimental data and the graph in (b) shows the sum of length squares $(\sum l_i^2 = (l^2 + l_m^2 + L^2))$ in mm^2 *vs.* time in s.

3 Conclusions

In summary, we have analyzed the imbibition dynamics in layered systems. In a two-layered porous medium, the fluid front in the smaller permeability layer always leads, which is in concurrence with the results of Bico and Quéré [21]. But for a layered system, the sum of squares of volume imbibed in individual layers is proportional to time, unlike described by Bico and Quéré [21] that the $(Total \quad Volume)^2 \propto t$. In a three-layered porous medium, the positioning of the fluid front is highly dependent on the arrangement of the layers and their permeability with respect to each other. An anomalous behavior is seen: the leading front is in the medium permeability layer (k_m), if the medium (k_m) and the small (k) permeability layers are separated by the large (K) permeability layer and $d + d_m < D$. But, when $d + d_m > D$, the fluid front in the small (k) permeability layer leads. In all the cases, $\sum(Volume)^2 \propto t$. This can be used in designing new porous media for diagnostics, to study imbibition of fluids in naturally occurring porous media such as wood which helps in choosing a suitable coat to prevent decay and to analyze the recovery from fractured oil reservoirs where spontaneous imbibition is important.

We acknowledge the financial support granted by the Indian Institute of Technology Delhi (Project No. MI01054).

Author contribution statement

JP and SSB designed the research. SA performed the experiments. SA and JP developed the model. GV assisted in data analysis. SA prepared the figures. SA, JP, and SSB drafted the manuscript. All authors reviewed the manuscript and gave final approval for publication.

References

1. C. Nicolaides, B. Jha, L. Cueto-Felgueroso, R. Juanes, Water Resour. Res. **51**, 2634 (2015).
2. L. Chaudhari, N. Hadia, S. Mitra, M. Vinjamur, Energy Sources, Part A: Recovery Util. Environ. Eff. **33**, 948 (2011).
3. M.A. Celia, S. Bachu, J.M. Nordbotten, K.W. Bandilla, Water Resour. Res. **51**, 6846 (2015).
4. M.T. Elenius, S.E. Gasda, in *Computational Methods in Geologic CO2 Sequestration*, Adv. Water Resour. **62**, Part C, 499 (2013).
5. K. Tang, K. Chau, C. Kan, J. Fan, Sci. Rep. **5**, 9689 (2015).
6. A. Attou, G. Ferschneider, Chem. Eng. Sci. **54**, 5031 (1999).
7. N.S.K. Gunda, M. Singh, L. Norman, K. Kaur, S.K. Mitra, Appl. Surf. Sci. **305**, 522 (2014).
8. R. Lucas, Colloid Polym. Sci. **23**, 15 (1918).
9. E. Washburn, Phys. Rev. **17**, 273 (1921).
10. D. Shou, L. Ye, J. Fan, Appl. Phys. Lett. **104**, 231602 (2014).
11. M. Kitron-Belinkov, A. Marmur, T. Trabold, G.V. Dadheech, Langmuir **23**, 8406 (2007).
12. G. Mason, N.R. Morrow, J. Colloid Interface Sci. **141**, 262 (1991).
13. M. Reyssat, L. Courbin, E. Reyssat, H. Stone, J. Fluid Mech. **615**, 335 (2008).
14. J. Gorce, I. Hewitt, D. Vella, Langmuir **32**, 1560 (2016).
15. M. Hultmark, J.M. Aristoff, H.A. Stone, J. Fluid Mech. **678**, 600 (2011).
16. A. Budaraju, J. Phirani, S. Kondaraju, S.S. Bahga, Langmuir **32**, 10513 (2016).
17. S. Chibbaro, Eur. Phys. J. E **27**, 99 (2008).
18. F. Diotallevi, L. Biferale, S. Chibbaro, G. Pontrelli, F. Toschi, S. Succi, Eur. Phys. J. ST **171**, 237 (2009).
19. J. Bear, *Dynamics of Fluids in Porous Media*, Vol. **1** (American Elsevier, New York, 1972).
20. M. Reyssat, L.Y. Sangne, E.A. Van Nierop, H.A. Stone, EPL **86**, 56002 (2009).
21. J. Bico, D. Quéré, Europhys. Lett. **61**, 348 (2003).
22. M. Dong, F. Dullien, J. Zhou, Trans. Porous Media **31**, 213 (1998).
23. D. Quéré, Europhys. Lett. **39**, 533 (1997).
24. S. Das, P.R. Waghmare, S.K. Mitra, Phys. Rev. E **86**, 067301 (2012).
25. S. Das, S.K. Mitra, Phys. Rev. E **87**, 063005 (2013).